



# RESERVOIR FACIES CHARACTERIZATION AND HETEROGENEITY ASSESSMENT IN AKOS FIELD, COASTAL SWAMP BELT, NIGER DELTA

MUHYIDEEN, H.\*, JOLLY, B.A., ABUBAKAR, R., ISIAKA, I.A., AND ABUBAKAR, M.T.

Department of Geology, Ahmadu Bello University, Zaria, Nigeria

## ABSTRACT

The quality of hydrocarbon reservoirs is determined by the level of heterogeneity inherent within the reservoir. A good quality reservoir should be less heterogeneous in terms of its porosity and permeability distribution. These parameters can easily be obtained from outcrop, core or well log data – whose access can be very limited. Thus, a more effective way of analyzing reservoir heterogeneity is through modelling which can reveal the spatio-temporal distribution of heterogeneity on a field-scale beyond well/outcrop locations. This study adopts a broader-scale methodology, incorporating seismic and well data to model reservoir heterogeneity across the Akos Field within the Coastal Swamp Belt of the Niger Delta. Results from this study show an accurate prediction of the spatial and temporal variation in heterogeneity across the Akos Field. In essence, our result shows variation in reservoir facies, porosity and permeability across the field. Porosity and permeability range from fairly good to excellent, with diagenetic and structural elements identified as controlling factors. The degree of heterogeneity was also quantified on the Dykstra-Parsons and Lorenz heterogeneity coefficient scales – with results showing degree of heterogeneity of 0.47% to 0.56% and 0.62% to 0.68% respectively. This study has provided significant insight into the heterogeneity distribution within the reservoir facies of Akos Field, and can serve as reference for reservoir characterization within the Coastal Swamp Belt in general.

**Keywords:** Akos Field, Heterogeneity, Niger Delta, Permeability, Reservoir facies, Porosity

**\*Correspondence:** muhyideenhamza@gmail.com, 08139136347

## INTRODUCTION

Reservoir heterogeneity holds a determining role in influencing reservoir production, recovery processes, and effective reservoir management [1, 2]. This encompasses variations in lithofacies, including mineralogical and genetic attributes associated with them. The degree of lithofacies heterogeneity significantly impacts volumetric and recovery factors across diverse reservoir types [3]. Heterogeneity is observed at various scales, ranging from microscopic petrophysical variations to mesoscopic lithofacies variability, macroscopic formation distribution, and megascopic basin-scale features [2, 4, 5]. Analyzing the variation in heterogeneity across a field or region, will require detailed collection of data from so many wells – which are not easily available. A cost-effective way of analyzing reservoir heterogeneity using limited available well and seismic data, is through modelling which can reveal the spatio-temporal distribution of heterogeneity on a field-scale beyond well/outcrop locations. Thus, the primary objective of this study is to integrate seismic and well log data to delineate reservoir lithofacies variations and associated heterogeneity within the reservoir units of Akos Field. The study also provided insights into factors controlling heterogeneity distribution within the study area.

## DATA AND METHODS

### Dataset

This study utilized high-resolution 3D seismic data and well logs from seven wells in the Akos Field, Niger Delta. The well logs included gamma-ray, resistivity, neutron-density, and check shot data integrated to delineate the lithofacies variation (heterogeneity) across the study area.

### Methods

Logs from seven wells were analyzed qualitatively and quantitatively to validate petrophysical parameters, lithofacies, and property variations in the field. Reservoir property maps including porosity, permeability [6] and water saturation were generated for purpose of the model. In this study, we use three-dimensional stochastic model and the Dyckstral-Parson and Lorenz heterogeneity coefficients for reservoir heterogeneity analysis. Lithological discrimination and pay zone delineation was done using Gamma and Resistivity log motif analysis. Nonlinear equations were used for determining volume of shale (Vsh) [7] was adopted for this study (see equation 2.2).

$$V_{shgr} = \frac{Gr_{log} - Gr_{clean}}{Gr_{clay} - Gr_{clean}} \quad \text{Linear [8] .....2.1}$$

$$V_{shSt} = \frac{V_{shgr}}{3.0 - 2.0 V_{shgr}} \quad \text{Nonlinear (Steiber).....2.2}$$

Since the nonlinear Vsh anticipated a lesser amount of shale, it was employed. Total porosity value was estimated using the root mean square approach as seen in equation 2.5 [9], as its often the scenario when the interval of interest is a hydrocarbon bearing reservoirs, while the density porosity was estimated from equation 2.3 [9].

$$\phi_d = \frac{2.65 - \rho_b}{2.65 - \rho_r} \dots\dots\dots 2.3$$

$$\phi_{nd} = \sqrt{\frac{\phi_n^2 + \phi_d^2}{2}} \dots\dots\dots 2.4$$

Hence, Effective porosity  $\phi_e$  was subsequently estimated from the total porosity using equation 2.4.

$$\phi_e = \phi_r - Vsh \cdot \phi_r \dots\dots\dots 2.5$$

Where;  $V_{shgr}$  = volume of shale gamma (linear),  $Gr_{log}$  = gamma ray log reading in zone of interest corrected for borehole size,  $V_{shst}$  = volume of shale (Steiber nonlinear),  $Gr_{clean}$  = gamma ray log reading in 100% clean zone,  $\phi_d$  = density porosity,  $Gr_{clay}$  = gamma ray log reading in 100% shale,  $pb$  = density log reading of zone interest,  $pf$  = density log reading for 100% water,  $\phi_n$  = Neutron porosity,  $\phi_{nd}$  = neutron-density porosity,  $\phi_r$  = total porosity.

The effective porosity against shale volume plot was used to determine the shale model, which was then compared with the plot guide [10]. The figures demonstrate that there is distributed shale in both reservoir sands. Due to this, the Hanai-Bruggeman [8] For determination of water saturation,  $S_w$ , equation 2.6, was adopted.

$$S_w = \frac{-B - \sqrt{B^2 + 4 \cdot H \cdot R_{rn} \cdot (R_t - R_{rn})}}{2 \cdot \phi \cdot R_{rn}} \dots\dots\dots 2.6$$

Using Schlumberger Petrel (2017), Well-to-seismic data tie was done (Figure 1) through the careful integration of the generated velocity model and synthetic seismogram to delineate geological events that correspond to the top and bottom of the mapped reservoirs on the seismic cube which show a relatively good tie (Figure 1). This was accomplished by convolutionally combining a zero-phase wavelet with the obtained reflectivity series as presented by the Zeoppritz [11] reflectivity mathematical equation (Eq. 2.7)

$$R = \frac{Z_2 - Z_1}{Z_2 + Z_1} \dots\dots\dots 2.7$$

where  $R$  = Reflection Coefficient,  $Z_1$  = Acoustic impedance of the overlaying layer,  $Z_2$  = Acoustic impedance of the layer below. Seismic surfaces (reservoir Horizon) were mapped and depth-structural maps were produced. model grid cells were defined to capture vertical and horizontal heterogeneity. Well log data were upscaled to match model grids and were validated. Property models was developed for facies, water saturation, clay volume, and effective porosity. These models were constructed to align with reservoir characteristics and were overlaid onto the facies models. Sequential Gaussian simulation and Kriging [12, 13], was used to estimate attribute values distribution across the reservoir area. Meanwhile variograms analysis was done for representative facies, petrophysical properties distribution and statistical parameters, including azimuth, dip, lag count, search radius, bandwidth, tolerance angle, and lag tolerance.

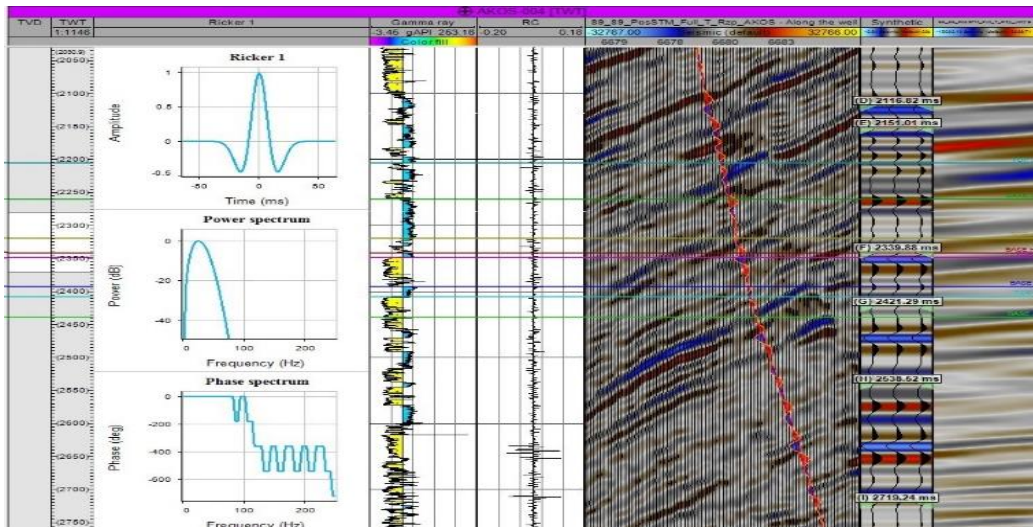


Figure 1: Seismic to well tie panel illustrating relatively good tie across the field.

**Geological setting and the study area.**

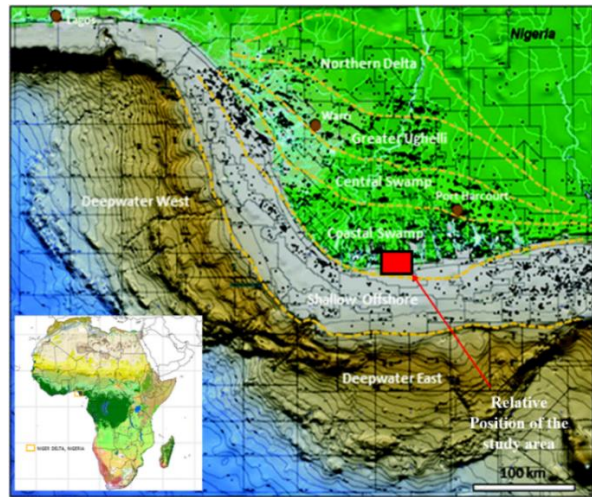
The Akos Field is situated in the southernmost sector of the Tertiary Coastal Swamp Belt of the Niger Delta Basin. Owing to confidentiality agreement and proprietary considerations, the precise geographical coordinates of the field have not been disclosed. However, the approximate location of the Akos Field is as illustrated in the map of the Niger Delta (Figure 2). The Niger Delta is a large regressive delta located in the Gulf of Guinea, covering an area of approximately 300,000 km<sup>2</sup> with sediment volume of 500,000 km<sup>3</sup> and thickness exceeding 10 km across the basin depositional centers [14, 15, 16]. It is known for its significant petroleum resources, ranking twelfth globally in terms of oil reserves [17, 18]. Stratigraphically, the delta consist of three formations (Figure 3) that are diachronous in nature – the Akata Formation at the base consisting of shale sequences and serving as a source rock [15, 19, 20]; the Agbada Formation which is stratigraphically above the Akata Shale, and characterized by intercalations of sand, and shale layers, which constitute the real deltaic component and is heavily faulted, and described with various fault types depending on the region in the delta [9]; and the Benin Formation which overlays the Agbada Formation, consists of large, porous, unconsolidated freshwater-bearing continental sediments, including alluvial and upper coastal-plain deposits up to 2000 m thick [9]. Structurally, the Niger Delta Basin is divided into zones which include the extensional zone on the shelf, the mud diapirs zone, the detachment fold zone, the inner fold and thrust belt, the translational zone, and the outer fold and thrust belt [21]. Several works have been carried out within the Niger Delta [22, 23, 24, 25] and the Akos Field region in particular. Some of these works include studies on sequence stratigraphy [27], pore pressure prediction analysis [28], comprehensive seismic and petrophysical attribute analysis [25, 26, 29, 30, 32], volumetrics [31] including three-dimensional static reservoir models [33]. These collective researches have greatly enhanced our knowledge of the geology and hydrocarbon potential of the Akos Field. However, detailed lithofacies heterogeneity studies which include petrophysical property variability and controls have not been comprehensively documented within the study area thus forming the basis for this study.

**RESULTS AND DISCUSSION**

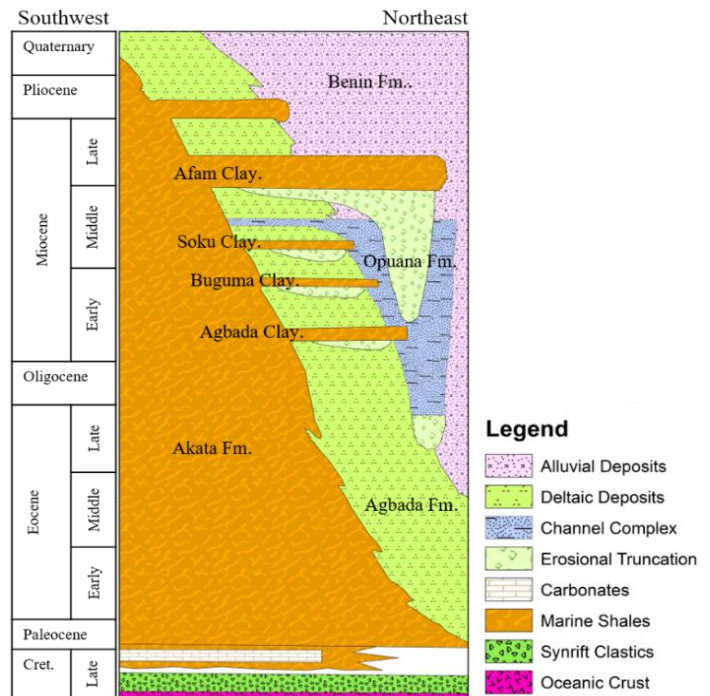
**Reservoir Facies**

Figure 4 is the result of reservoir correlation across the available wells in the study area. Here, two major reservoirs of interest (Reservoir H and J) were identified, mapped and analyzed for heterogeneity variation. Reservoirs H and J extend laterally across the wells (Figure 4). Reservoir H is positioned above

Reservoir J and occur at depth ranging from 8355 to 8912 feet across the field. It exhibits gross thickness variations within the range of 47 to 299 feet across the field. Reservoir J, which lies below Reservoir H, extends across all the wells and relatively show variation in both facies variation and gross sand thickness (Figure 4). This reservoir occurs at depth ranging from 8542 to 9938 feet and exhibits a gross thickness varying between 21 to 171 feet.



**Figure 2:** Map of Niger Delta showing the pproximate location of Akos Field.



**Figure 3:** Showing the lithostratigraphic section of Niger Delta (Modified from [16]).

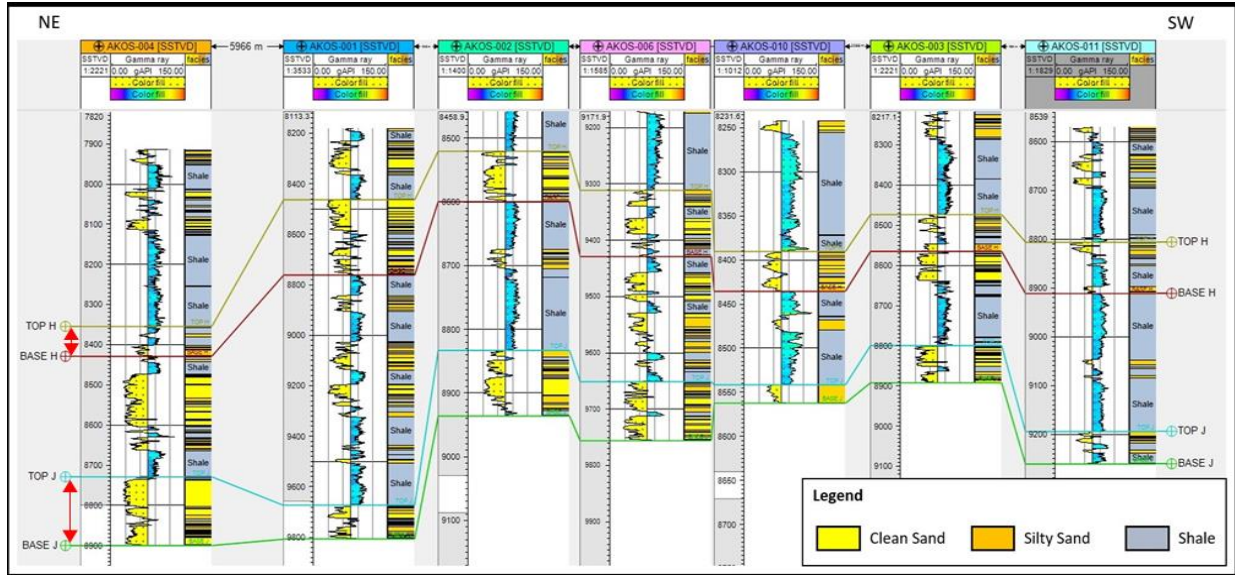


Figure 4: Showing well correlation of the studied Reservoir H and J

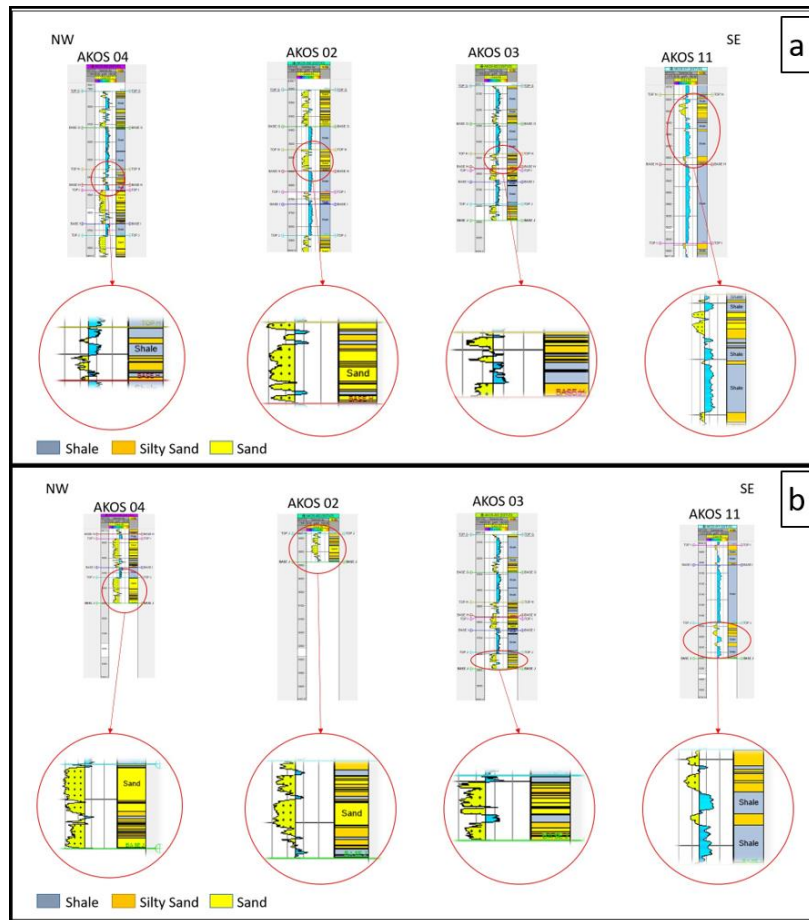
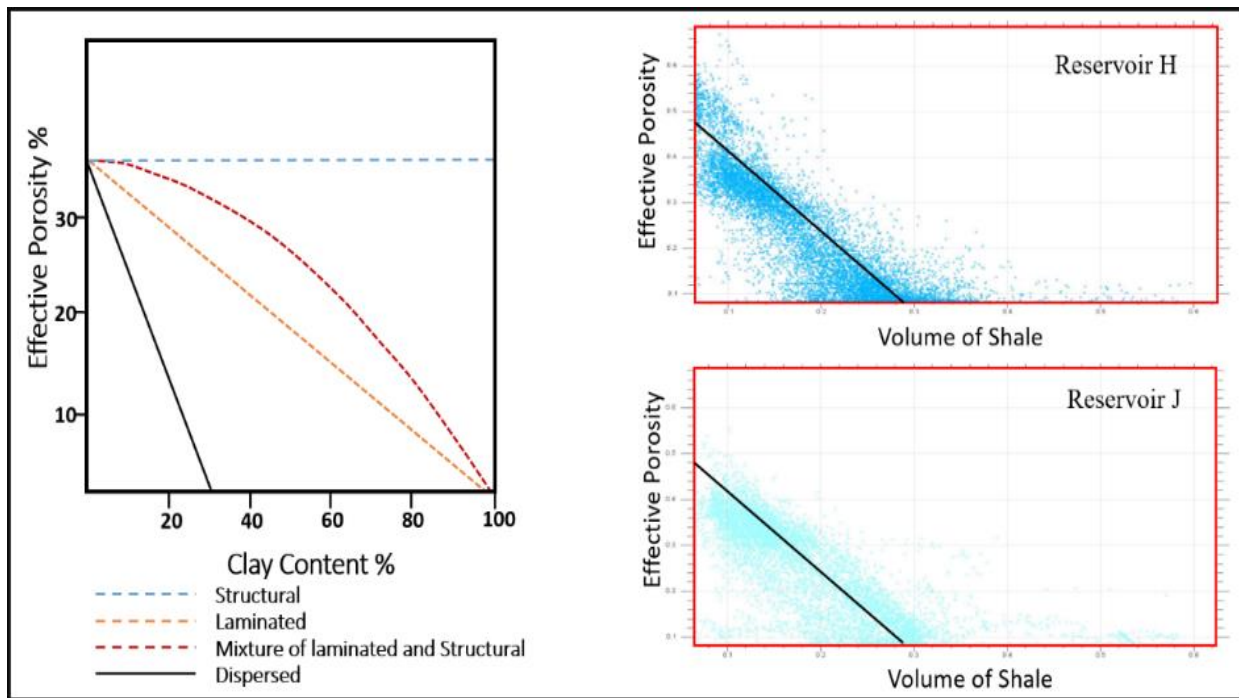


Figure 5: Facies vertical and lateral variation across the reservoirs. (a) Facies distribution down the wells within Reservoir H along NW-SE illustrating facies heterogeneity across the reservoir (b) Facies variation down the wells within Reservoir J similarly along same trend. Shales (grey) volume relatively increases while sand (yellow) otherwise dominant at Akos 2 and decreases at intervals towards the SE in the reservoir.

The Chevron reservoir characteristic plot (Figure 6) provides a visual representation of the relationship between effective porosity and clay concentration, which are critical factors for evaluating reservoir quality. This plot serves as a pivotal tool for predicting the clay type distribution present in a reservoir. Reservoirs "H" and "J" are situated within the region associated with dispersed clay types (Figure7). This implies that the effective porosity in reservoirs H

and J is influenced by the presence of fine-grained clay particles (Autogenic clays) distributed across the rock matrix, which has notable impact both on porosity and permeability across Reservoir H and J as they occupy pore spaces and lead to pore blockage as suggested by [34, 35]. Consequently, this reduction in overall porosity affects the reservoir's storage capacity and fluid mobility, which ultimately impacting production rates and recovery efficiency.



**Figure 6:** Chevron Reservoir Characteristic plot of effective porosity and clay content of Reservoir H and J showing suggesting dispersed types of clay distribution in the reservoirs [36].

**Structures and reservoir facies distribution.**

Figure 7a is a Root Mean Square attribute map on a time-slice at depth of 2227ms showing mapped faults. These faults were categorized into groups: listric faults (F1, F2, F3, F4, and F5), synthetic and antithetic faults (F3 and F2), and back-to-back faults (F1 and F6) as shown in Figure 7b. These faults extend vertically through Reservoirs H and J. Although the major faults (F1, F2, F3, F4 and F5) generally have an approximately East-West (E-W) orientation, they are accompanied by various sub-parallel types (Figure 7b). While fault displacements appear relatively small, they interact with sediment supply during deposition, leading to variations in seismic facies thickness across the faults and along the hanging walls of the faults. High amplitude facies

(sands) appear to be distributed along the hanging wall of the mapped faults (e.g., Fault 1; Figure 7a and 7b). The variations and alignment of high amplitude sands along the faults plane suggest the various changes in complex interaction between the sediment supply and the consistent accommodation created by the syndepositional fault movement over time. This syndepositional fault movement must have controlled sediment supply and as a consequence, must have impacted on reservoirs and hence influenced the overall heterogeneity. Figure 7c shows a seismic section illustrating the syndepositional fault interaction evident in the seismic facies packages forming a subtle anticlinal structure (rollover anticline) along the fault.

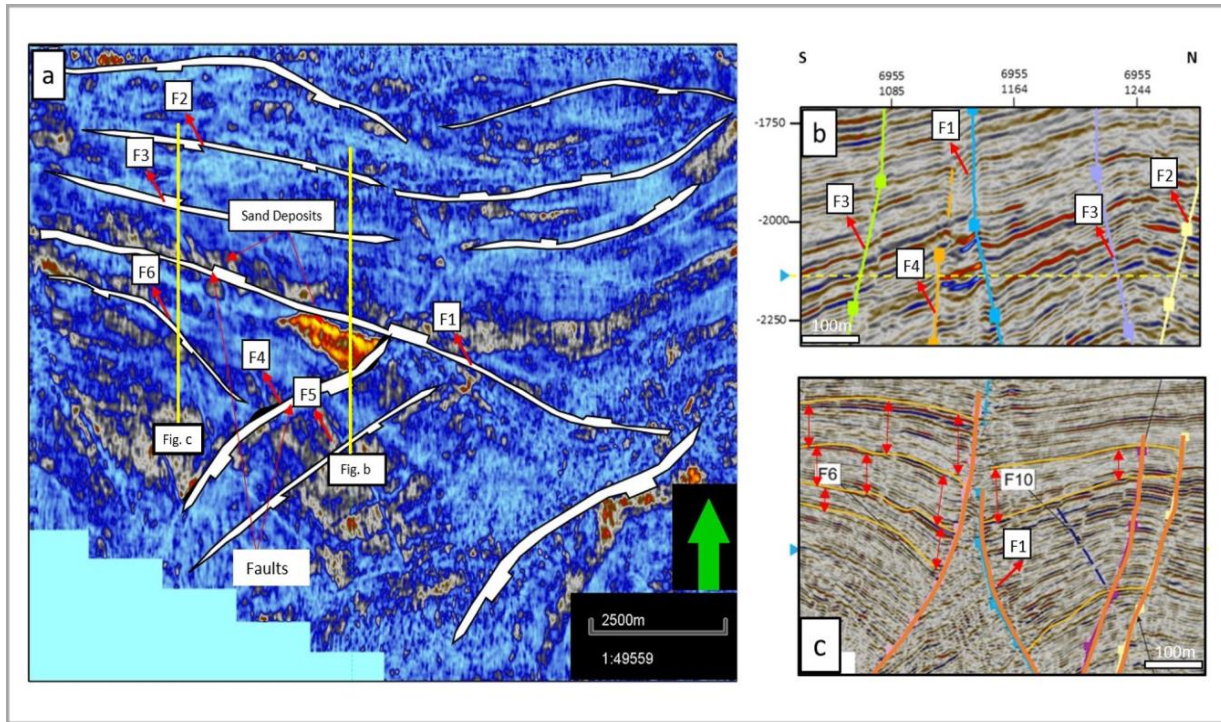


**Figure 7:** Faults configuration and interaction in the reservoir region of the study area (a) A Root Mean Square attribute time slice showing the distribution of faults and their interaction with high amplitude sand deposit within the reservoir area. (b) Seismic section (see location on Figure 7a) showing the distribution of high amplitude sands around the fault plane of the fault’s blocks. (c) Seismic section (see location on Figure 7a) illustrating syndepositional faults interaction with deposited package in the study area.

**Petrophysical parameters for Reservoir H and J.**

Table 1 displayed below, provides an illustration of the relative heterogeneity observed in the petrophysical properties across Reservoir H along the same trend (approximately E-W). Reservoir H Porosity values ranges from 0.13% to 0.22%, and permeability values ranges from 560 to 1750 mD, as detailed in Table 1. The estimated Shale volume ( $V_{sh}$ ) for Reservoir H varies

between 21% and 37%, while the water saturation ( $S_w$ ) ranges from 32% to 45% across the wells. Reservoir J shows porosity values ranging from 0.12% to 0.21% and permeability values ranges from 665 to 1675 mD. Additionally, the shale volume ( $V_{sh}$ ) varies from 16% to 41% across the wells ultimately showing the various heterogeneity variation across the reservoirs.

**Table 1:** The heterogeneity distribution of various reservoir properties across the study reservoirs.

Reservoir Facies	Thickness (ft.)	Permeability (mD)	Porosity	Volume of Shale	Dykstra-Parson’s Permeability Heterogeneity	Lorenz Coefficient of Heterogeneity
H	47 - 299	560 - 1750	0.13 - 0.22	0.21 - 0.37	0.56	0.47
J	21 - 171	665 - 1416	0.12 - 0.21	0.16 - 0.41	0.68	0.62

**3D Stochastic Model and Heterogeneity Distribution.**

Figures 8 to 11 present comprehensive 3D reservoir models representing Reservoirs H and J. These models effectively illustrate the lithofacies and v petrophysical variations within these reservoirs, including facies,

porosity, permeability, and water saturation, all of which play pivotal roles in characterizing these reservoirs. In the southern part of Reservoir H, as shown in Figures 8 and 9, facies models reveal a prevalence of coarse sand facies interspersed with thin shale layers. Towards

reservoir H central area, fine-sand facies dominate, while the northern and southern portions consist of finer facies, ranging from shale to silty-shale (Fig. 9a). Porosity and permeability distribution (Figure 9b and 9c) across Reservoir H model displays a pattern of relatively good to excellent values, with permeability exhibiting lower heterogeneity. Conversely, porosity exhibits excellent characteristics in the eastern and northwestern sections with a lower porosity in the southeastern part. Overall, the heterogeneity in Reservoir H becomes more pronounced as one moves towards the northeastern region of the field. Across Reservoir J, the facies and petrophysical models (Figures 10 and 11) indicate that this reservoir is primarily dominated by sands, ranging from fine to

coarse facies, in the western region, with some shale patches in the northern and northeastern part of the reservoir. Reservoir J exhibits more consistent properties across the reservoir. In general, the observed heterogeneity in both Reservoirs H and J appears to be relatively consistent, suggesting a similar reservoir condition. This consistency is further supported by their spatial and temporal proximity within the field and the distribution of petrophysical properties across the field. Table 1 above summarizes the distribution of petrophysical heterogeneity parameters across Reservoirs H and J respectively.

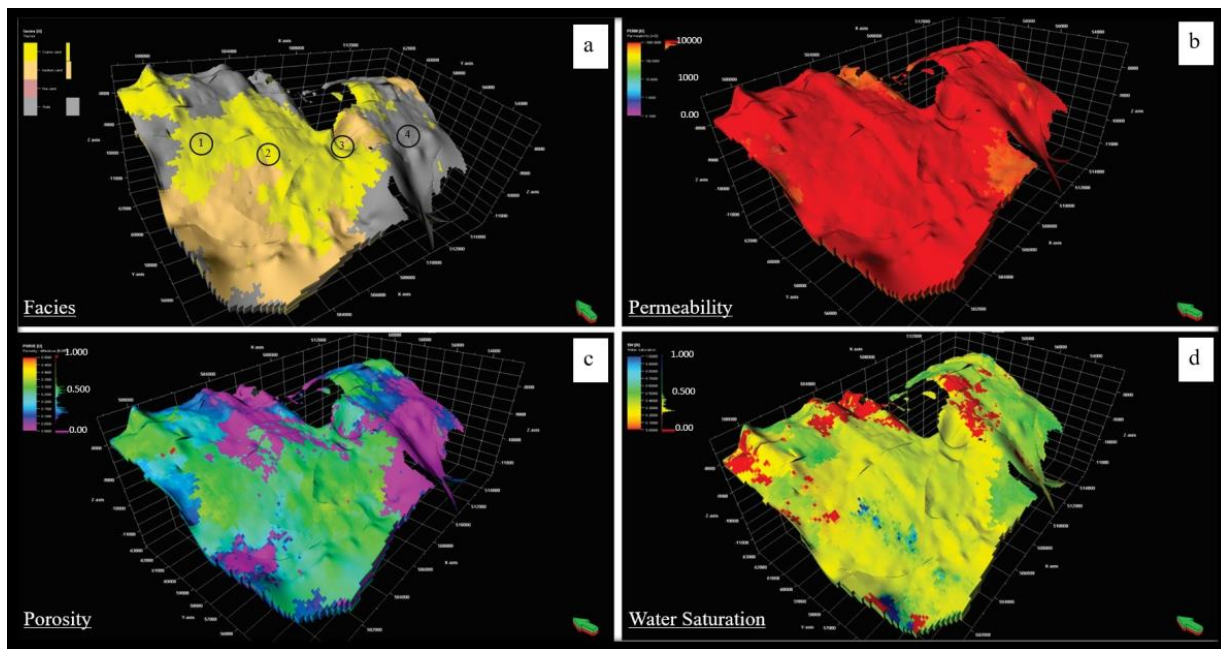


**Figure 8:** 3D geostatistical model of Reservoir H showing the spatio-temporal variation of the petrophysical properties across the flow unit. (a) Illustrates the spatio-temporal distribution of facies identified in the reservoir (see legend). This reservoir is spatially dominated by sands and silty-sands with patches of shale at the eastern part. (b) Illustrate the permeability distribution of reservoir H, which suggest a good to excellent permeability express as red to orange colour across the model (c) Illustrates porosity across the reservoir and reflect an average to good porosity across the flow unit. Porosity values are express in green to blue (high porosity), and purple (low porosity) and. (d) represents the water saturation in the fluid column and follow flows with other petrophysical parameters such as porosity. Note: b, c, and d, are dependable and consequential to their corresponding facies model. 1= Akos 4 well, 2 =Akos 2 well, 3=Akos 3 well and 4=Akos 11 well respectively.

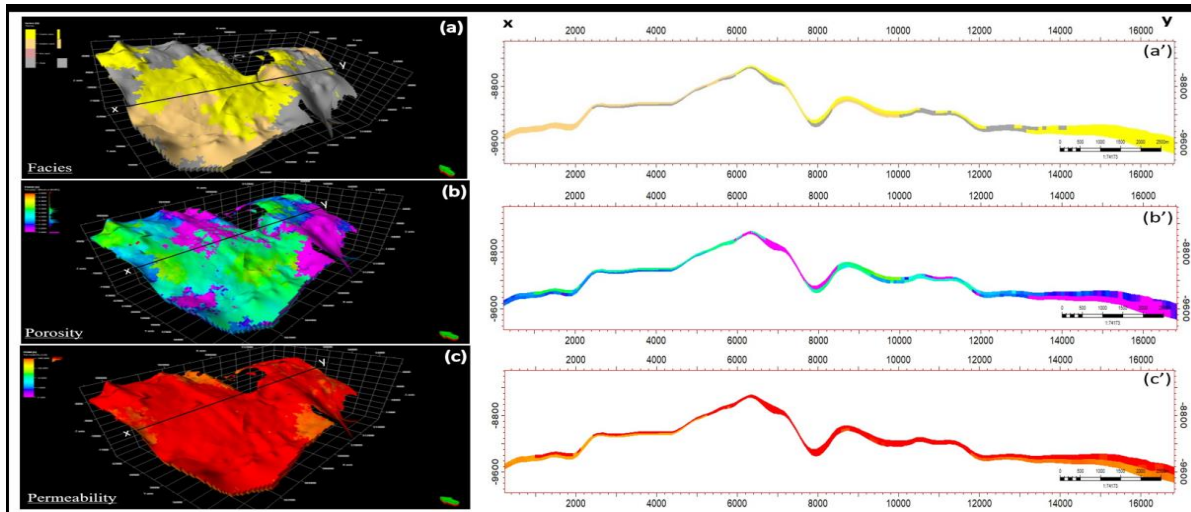


**Figure 9:** Cross sectional view of Reservoir H model and the heterogeneity distribution across the reservoir along x-y trending approximately E-W of the study area. (a) represents a facies profile along x-y, with relatively stratified shale at the mid-western and eastern part of the profile against the dominated sand and silty sand across the reservoir. (b) shows the porosity profile in the reservoir with apparently low porosity toward the middle from the eastern part of the profile (i.e y toward x). (c) is showing permeability which follows approximately similar suit across the model. (purple = lower porosity, blue to green= increasing porosity).

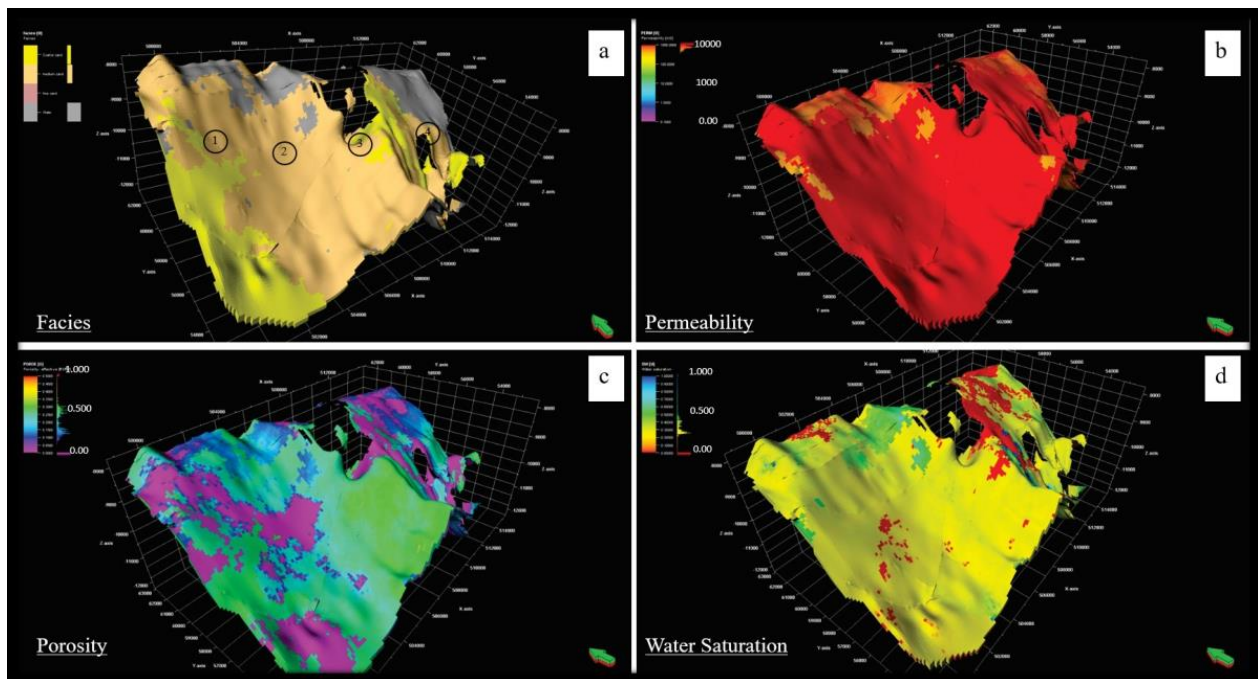


**Figure 10:** 3D geostatistical model of Reservoir J Spatio-temporal variation of its petrophysical character across the flow unit. (a) Illustrates the spatio-temporal distribution of facies identified in the reservoir. This depicts a less heterogeneous reservoir with patches of shaly sands at the northern flank. (b) Illustrate the permeability distribution of the reservoir, which suggests a good to excellent permeability character. (c) Illustrates porosity across the reservoir which reflect an average to good porosity; Blue to green depicts relatively high porosity while purple depicts a relatively low porosity area. (d) shows water saturation concentrated in patches, supporting evidence for inhomogeneous in the area. all petrophysical models are conform on the facie heterogeneity in the area. 1= Akos 4 well, 2 =Akos 2 well, 3=Akos 3 well and 4=Akos 11 well respectively.

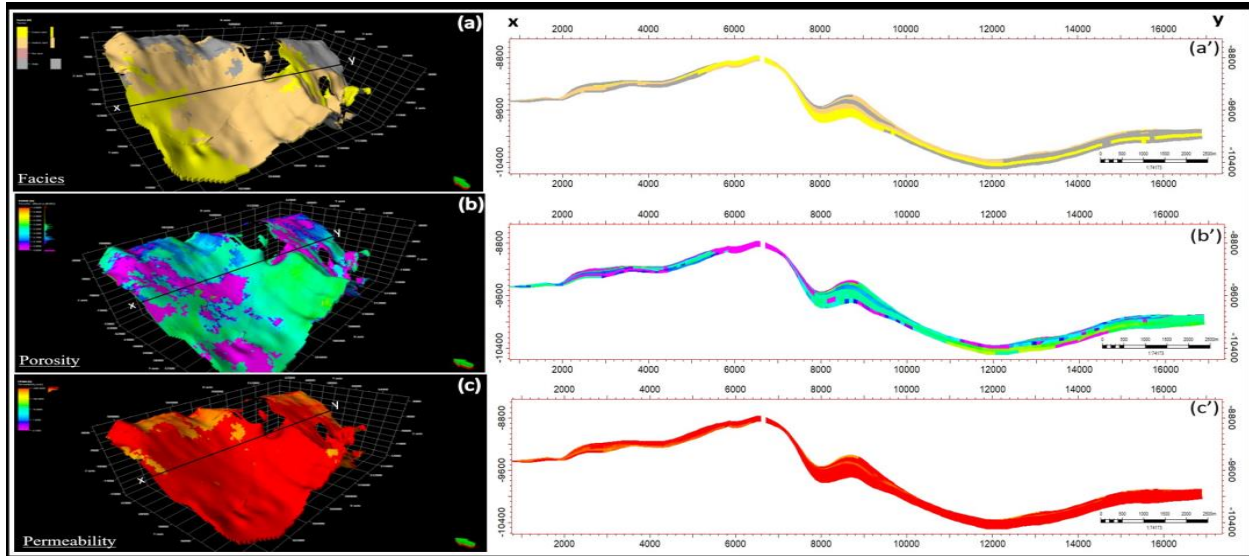


**Figure 11:** Cross sectional view of Reservoir J and the heterogeneity distribution across the reservoir along x-y trending approximately E-W of the study area. (a` ) represents a facies profile along x-y, with relatively clean sand at the middle area and the eastern part of the profile against the dominated shale to silty-shale at the eastern bottom and the western part of the profile. (b` ) shows the porosity profile in the reservoir with apparently high heterogeneity, characterized as patches of low porosity area (purple) at the mid to western part of x-y. (i.e. y toward x). and blue to green at the other part, reflecting a better porosity area (c` ) is showing permeability which follows approximately similar suit across the model especially with the porosity model. (purple = lower porosity, blue to green= increasing porosity).

In an attempt to quantitatively assess the degree of heterogeneity distribution within the target reservoirs, namely Reservoirs H and J, in the study area, we employed the Dykstra-Parsons permeability variation analysis. The Dykstra-Parsons permeability variation results for Reservoirs H and J reveal a notable degree of heterogeneity, with Dykstra-Parson’s permeability values of 0.56 and 0.68, accompanied by corresponding Lorenz Coefficient values of 0.47 and 0.62, respectively. Heterogeneity, in this context, spans the spectrum from 0 (homogeneity) to 1 (complete heterogeneity) on both the Dykstra-Parsons Permeability and Lorenz Coefficient scales, denoted as  $0 < L < 1$  and  $0 < V < 1$ . A summary of the Dykstra-Parsons and Lorenz heterogeneity values for the reservoirs in our study area is presented in Table 1, reaffirming that the Dykstra-Parsons and Lorenz heterogeneity variations within the field fall within the range of 0 to 1, signifying their heterogeneous nature which class on a moderate heterogeneity reservoir type.

## CONCLUSION

The reservoirs of the Akos Field, situated within the Niger Delta Basin, has been characterized and variation in their heterogeneity was also assessed; thus, shedding light on the intricate nature of two payzones, namely

Reservoirs H and J. These reservoirs display diverse petrophysical characteristics, encompassing facies distribution, porosity, permeability, and shale volume. Results of spatio-temporal 3D geostatistical modeling show that the petrophysical properties across Reservoirs H and J are relative heterogeneous. This heterogeneity is primarily attributed to variability in lithofacies. The estimated average clay volume within the reservoir intervals stands at approximately 28%, placing them under the shaly-sand reservoirs type. With recorded average porosity and permeability values of 17% and 1090 mD, respectively.

This study revealed two main controls on the heterogeneity distribution within the Akos Field. These include the influence of sediment routing system and structural influence. Heterogeneity across Akos Field have been estimated to range from moderately to strongly heterogeneous with Dykstra-Parson and Lorenz heterogeneity coefficient values of 0.56-0.68 and 0.47-0.62. This study has significantly advanced our understanding of the reservoir heterogeneity and the genetic factors influencing their spatial distribution within the Akos Field of Niger Delta.

## COMPETING INTEREST DECLARATION

No conflicts of interest exist, according to the authors, with the publishing of this article.

## ACKNOWLEDGMENT

We extend our sincere appreciation to Shell for their invaluable contribution of data, which greatly facilitated and enriched our research efforts. Their support was instrumental in advancing our understanding and findings in this study.

## REFERENCES

1. MALUREANU, I.I. & BATISTATU, V.M. (2010). The analysis of reservoir heterogeneity from Well Log DATA. *Επιστημονική Επετηρίδα του Τμήματος Γεωλογίας (ΑΠΘ)*, **99**: 149-154.
2. MISHRA, S.K. (2004). Integration of Different Types of Data for Characterization of Reservoir Heterogeneity.
3. OKPOGO, E.U., ABBEY, C.P. & ATUEYI, I.O. (2018). Reservoir characterization and volumetric estimation of Orok Field, Niger Delta hydrocarbon province. *Egyptian journal of petroleum*, **27**(4): 1087-1094.
4. MATHERON, G. (1963). Principles of geostatistics. *Economic geology*, **58**(8): 1246-1266.
5. ODEDEDE, O. (2019). Reservoir heterogeneity of Agbada Formation sandstone from PZ-2 well and PZ-4 well, Niger Delta: implications for reservoir management. *Journal of Petroleum Exploration and Production Technology*, **9**: 997-1006.
6. CORBETT, P. & JENSEN, J.L. (1992). Estimating the mean permeability: how many measurements do you need?. *First Break*, **10**(3).
7. ASQUITH, G.B., KRYGOWSKI, D. & GIBSON, C.R. (2004). *Basic well log analysis* (Vol. 16). Tulsa: American Association of Petroleum Geologists.
8. BERG, C.R. (1996). Effective-medium resistivity models for calculating water saturation in shaly sands. *The Log Analyst*, **37**(03).
9. PATRICK, A.C., ORENUGA, I.A. & OKPOGO, E.U. (2018). Effect of shaliness on water saturation: A case study of TN Field Niger Delta. *Iraqi Journal of Science*, **59**(1C): 510-519.
10. OGBE, O.B., ORAJAKA, I.P., OSOKPOR, J., OMERU, T. & OKUNUWADJE, S.E. (2020). Interaction between sea-level changes and depositional tectonics: Implications for hydrocarbon prospectivity in the western coastal swamp depobelt, Niger Delta Basin, Nigeria. *AAPG Bulletin*, **104**(3): 477-505.
11. ZOEPFRITZ, K. & ERDBEBENWELLEN, V.I.I.B. (1919). On the reflection and propagation of seismic waves: *Gottinger Nachrichten*.
12. GOOVAERTS, P. (1997). Kriging vs stochastic simulation for risk analysis in soil contamination. In *geoENV I—Geostatistics for Environmental Applications: Proceedings of the Geostatistics for Environmental Applications Workshop*, Lisbon, Portugal, 18–19 November 1996 (pp. 247-258). Dordrecht: Springer Netherlands.
13. MANCHUK, J.G. & DEUTSCH, C.V. (2012). A flexible sequential Gaussian simulation program: USGSIM. *Computers & Geosciences*, **41**: 208-216.
14. HOSPERS, J. (1965). Gravity field and structure of the Niger delta, Nigeria, West Africa. *Geological Society of America Bulletin*, **76**(4): 407-422.
15. KULKE, H. (1994). with 17 figures. *Regional Petroleum Geology of the World: Africa, America, Australia, and Antarctica*, **30**, 143.
16. DOUST, H., OMATSOLA, E. Niger Delta// EDWARDS, J.D., SANTOGROSSI, P.A. *Divergent/passive margin basins: AAPG Memoir 48*. Tulsa: *American Association of Petroleum Geologists*, **1990**: 239–248.
17. FOREMAN, N.E. (1996) *Global production through 2005*. *World Oil* **217**.12.
18. KLETT, T.R., AHLBRANDT, T.S., SCHMOKER, J.W. & DOLTON, G.L. (1997). Ranking of the world's oil and gas provinces by known petroleum volumes (No. 97-463). US Dept. of the Interior, Geological Survey.
19. AVBOVBO, A.A. (1978). Tertiary lithostratigraphy of Niger delta. *AAPG Bulletin*, **62**(2): 295-300.
20. LUCAS, F.A. & FREGENE, T.J. (2018). Paleo-environmental reconstruction of oligocene to early miocene sediments of Greater UghelliDepobelt, Niger Delta Basin. *Journal of Applied Sciences and Environmental Management*, **22**(1): 99-102.
21. CORREDOR, F., JOHN, H.S. & FRANK, B. (2005). Structural styles in the deep-water fold and thrust belts of the Niger Delta. *AAPG Bulletin*, **89**(6): 753-780.

22. ADEOTI, L., ONYEKACHI, N., OLATINSU, O., FATOBA, J. & BELLO, M. (2014). Static reservoir modeling using well log and 3-D seismic data in a KN field, offshore Niger Delta, Nigeria.
23. ALEGE, T.S. (2017). Structural Interpretation of 3D Seismic Data of Akos Field in the Coastal Swamp Depobelt of the Niger Delta.
24. ALEGE, T.S. (2017). Structural Interpretation of 3D Seismic Data of Akos Field in the Coastal Swamp Depobelt of the Niger Delta.
25. OLUWOLE, D.O. & LAWRENCE, F.S. (2019). Effects Of Heterogeneity on The Petrophysical Parameters of Sandstone Reservoirs and Volumetrics In? Devo? Field, Niger Delta. Effects Of Heterogeneity on The Petrophysical Parameters Of Sandstone Reservoirs And Volumetrics In? Devo? Field, Niger Delta, **38**(1): 33-33.
26. ANYIAM, O.A., MODE, A.W. & OKARA, E.S. (2018). The use of cross-plots in lithology delineation and petrophysical evaluation of some wells in the western Coastal Swamp, Niger Delta. *Journal of Petroleum Exploration and Production Technology*, **8**: 61-71.
27. BASSEY, C.E. & FAGBOLA, O. (2002). Sequence stratigraphy of Iso field, western onshore Niger Delta, Nigeria. *Journal of Mining and Geology*, **38**(1): 43-48.
28. EMUDIANUGHE, J. (2019). Well-based pore pressure validation: a case study of Akos field, coastal depobelt, Niger Delta Basin. *FUPRE Journal of Scientific and Industrial Research (FJSIR)*, **3**(1): 104-111.
29. EMUJAKPORUE, G.O. & ENYENIHI, E.E. (2020). Identification of seismic attributes for hydrocarbon prospecting of Akos field, Niger Delta, Nigeria. *SN Applied Sciences*, **2**: 1-11.
30. HORSFALL, O.I. & NGERI, A.P. (2019). Structural Interpretation of Akos Field, Coastal Swamp Depobelt, Niger Delta, Nigeria. *Asian Journal of Applied science and Technology (AJAST)*, **3**(1): 68-77.
31. OMOKENU, E.G. & ENIFOME, E.E. Volumetric Analysis of Hydrocarbon Reservoirs in 'AKOS' Field, Niger Delta, Nigeria.
32. ONWUSICHINELO ET AL., (2017) Petrophysical ttributes and Reservoir Volumetrics In "Akos Field", Onshore Niger Delta, **6**(5): 601-614.
33. UMUKORO, A. G. & OKENGWU, K. O. (2022). Sequence stratigraphic framework of 'AKOS' field, Niger Delta. *Scientia Africana*, **21**(1), 133-148.
34. WILSON, M.D. & PITTMAN, E.D. (1977). Authigenic clays in sandstones; recognition and influence on reservoir properties and paleoenvironmental analysis. *Journal of Sedimentary Research*, **47**(1): 3-31.
35. WILSON, M.J., WILSON, L. & PATEY, I. (2014). The influence of individual clay minerals on formation damage of reservoir sandstones: a critical review with some new insights. *Clay minerals*, **49**(2): 147-164.
36. GUIDE. Sandstone Reservoir Evaluation: Sandstone Characteristics, presented at the Intermediate Formation Evaluation Seminar held in Ibadan, Nigeria. August (1996) 25 – 31, 1 – 44.